MODELING AND MAPPING WILDFIRE POTENTIAL IN MEXICO BASED ON VEGETATION AND DROUGHT CONDITIONS USING REMOTE SENSING AND GIS TECHNOLOGY

Franz Mora
Center for Advanced Land Management Information Technologies (CALMIT),
University of Nebraska-Lincoln. Lincoln NE, 68588
E-mail: mora@calmit.unl.edu

Gilberto Hernández-Cárdenas
Departamento de Biología,
Universidad Autónoma Metropolitana-Iztapalapa, México
E-mail: gilberto@calmit.unl.edu

ABSTRACT

An increasing severity in the occurrence of wildfires in Mexico has been recently associated with the activity of "El Niño" Southern Oscillation (ENSO). A spatio-temporal analysis of fire potential indicated that indeed, catastrophic fires could occur due to unusual droughts and dry fuel conditions during ENSO years. In order to evaluate the effects that ENSO may excerpt on fire activity; estimates of fire potential were calculated for several years using satellite imagery and climatic data, and implementing a probabilistic GIS fire model. Fire probability was calculated from multi-temporal vegetation information (derived from multi-temporal AVHRR-NDVI imagery), and drought conditions are derived from precipitation data. When applied to land cover data representing several years, the temporal trends of fire potential for the entire country were analyzed. This model is particularly useful for temporal analysis, and it has been partially validated by comparing fire locations and fire potential for the 1998-fire season.

Keywords: Fires in Mexico, GIS Fire potential Model, ENSO effects on vegetation.

INTRODUCTION

The occurrence of wildfires is still the most prominent factor of global change, by being directly associated with the production of greenhouse gases. Wildfires are greatly associated with land use change practices and deforestation, promoting the loss of green biomass and biodiversity (Andreae 1991, Hao and Liu 1994; Levine *et al.*, 1999).

During 1998, the occurrence of catastrophic wildfires increased considerably in Mexico. According with official statistics (SEMARNAP 1998), the number of fires between January and July alone (14,136) doubled the yearly average between 1992-1997 (7,121). As compared with previous years, the area affected (540,859 ha) was almost three times greater than the yearly average previously reported (176,718 ha). At present, land use conversion and deforestation threaten most of the areas affected by fires (SEMARNAP 1998). The most important factor associated with the worst fire season was probably "El Niño" Southern Oscillation (ENSO).

Even when there was a strong indication that drought conditions associated with ENSO triggered the problem of the 1998 catastrophic fires, it is still unclear how patterns of inter-annual climate variations interact with vegetation activity to create severe fire conditions. Unfortunately, the occurrence of ENSO events in determining severe drought conditions for fire development is just beginning to be understood. Nevertheless, it is necessary to know how ENSO events can modify patterns or regional fire potential, in order to anticipate future drought scenarios.

The occurrence of catastrophic fires, especially at regional scales, is a matter of great concern because they not only threaten human life and property, but also severely damage natural resources where fire is not a recurrent perturbation factor. In areas like the tropical rainforest, wildfires represent an additional threat for loss of biodiversity, as the occurrence of catastrophic events jeopardizes the conservation of natural habitat and makes necessary the implementation of management plans for restoration with resources that, otherwise, could be allocated for preservation purposes.

Traditionally, fires in Mexico that occur in natural areas are predominantly human induced (SEMARNAP 1998). Most of these are the result of agricultural practices. Even when there is a great controversy in using fire as a management tool for agricultural purposes, their impacts can be ameliorated if estimates of regional fire potential are known in advance. The knowledge of drought events as related with vegetation conditions and fire potential can be used to make management recommendations. The 1998 fire season was exceptional, and fire activity observed that particular year makes it important to evaluate the probability of fire occurrences under similar scenarios, especially within a global change framework, where ENSO events are more likely to occur.

The interaction of traditional land use practices with adverse ecological conditions, especially those related with agricultural burns and slash-and-burn-agriculture, may have also played a role in determining the severity of fires during 1998. However, defining into what extent wildfires that occurred that year were driven by inter-annual climatic variability, and on the other hand, into what extent were they promoted by agricultural and land use practices (especially in tropical areas) is still matter of great debate. From the regional point of view, fire science in Mexico is undeveloped. In general, fire statistics are underestimated and fire potential is not evaluated on scientific basis. This situation is complicated by the fact that fire information is not available for regional analysis. It is therefore necessary to develop new tools to address issues like this for the country.

Satellite information is the most promising tool for evaluation, as it can provide an important contribution to the understanding of the effects of fires in the environment. With satellite imagery, fire occurrences can be consistently monitored, and comprehensive historical data sets can be created. Fire danger and hazards can be evaluated by looking simultaneously to both, fire occurrence and vegetation condition (Barbosa *et al*. 1999; Belward *et al*., 1995; Ehrlich et al., 1997; Hugh and Lambin 1998).

Moreover, alternative sources of regional information are necessary to evaluate forest potential and risk. Presently, the use of remotely sensed data and geographical information system (GIS) technology is widely used for landscape analysis and drought conditions (Reed 1993). GIS technology offers the alternative to consistently evaluate fire incidence, fire potential and fire history at regional levels, by integrating satellite imagery and several ancillary sources of information necessary to implement spatial fire models (Chuvieco and Congalton 1989; Chuvieco and Martin 1994). It can also be used for the evaluation of possible scenarios, as well as to provide cartographic resources for planning decisions (Chuvieco and Salas 1996).

The purpose of this paper is to present a methodology for implementing a fire potential model for evaluation purposes in Mexico, by integrating satellite imagery and climate data into a GIS. In addition, the methodology proposed here is used to analyze spatial and temporal patterns of fire potential, as associated with ENSO events in order to identify potential relationships. The temporal analysis of fire potential and vegetation condition is based on satellite data representing the driest month of the year for almost two decades. This GIS model is conceptualized as a tool to evaluate the temporal and spatial patterns of fire potential, and to identify potential fire risk scenarios as a result of inter-annual variations in climate and vegetation.

METHODS

A model is presented here to evaluate historical fire potential based mostly on satellite imagery and ancillary geographic data. This is a probabilistic model, integrated into a geographical information system (GIS) that evaluates fire potential scenarios. Fire probability is based on vegetation condition and drought, and the variations observed due to inter-annual variability in climate and vegetation (Figure 1). This GIS model can be implemented at several spatial scales in Mexico.

The GIS model calculates the natural probability of a fire occurrence in the landscape, based primarily on the vegetation and drought condition. The temporal and spatial patterns of potential fuels are evaluated by using multi-temporal information of vegetation activity. The drought condition for fire development is evaluated when climatological data is used. In addition, the model can be modified to evaluate "what if" scenarios when ancillary land use data is included into the GIS.

The GIS model is based on significant deviations from normal conditions to calculate the probability of a fire. The probability of a fire is calculated when both, the drought and vegetation conditions are of such magnitude that probability to produce a fire increases dramatically. The fire probability is calculated using GIS map algebra as:

$$FP = PFVC + PFD - PIND \quad (1)$$

Where:

FP = Fire probability (%) based on drought conditions and vegetation condition.

PFVC = Fire probability based on the relative vegetation condition (%). Fire probability equals one when the vegetation condition is a 100% deviation from optimal vegetation conditions; and 0 when the vegetation condition equals the optimal vegetation condition.

PFD = Fire probability according with drought conditions (%). Fire probability equals one when the precipitation amount is a 100% deviation from the normal; and 0 when the precipitation amount equals the normal.

PIND = Probability that both events are independent (%).

In essence, the model (1) integrates the effects of vegetation condition (greenness) and adverse climate conditions (droughts) and calculates the probability of a fire only when both events occur simultaneously.

The PFD is evaluated as a measure of precipitation variability by calculating the coefficient of precipitation variation (CPV), which is a deviation from normal precipitation conditions (i.e., the long-term average). In other words, PFD determines the climatological probability of a fire based on drought condition as:

Where:

$$CPV = [P_{mean} / P_{std}] * 100 \quad (2)$$

CPV = Coefficient of precipitation variation, in percent.

P_{mean} = The mean value between the observed precipitation and the “normal” precipitation value.

P_{std} = The standard deviation value between the observed precipitation and the “normal” precipitation.

Then, the values in (2) indicate that the greater the deviation from “normal” precipitation conditions, the greater probability of a drought. The climatic prob-

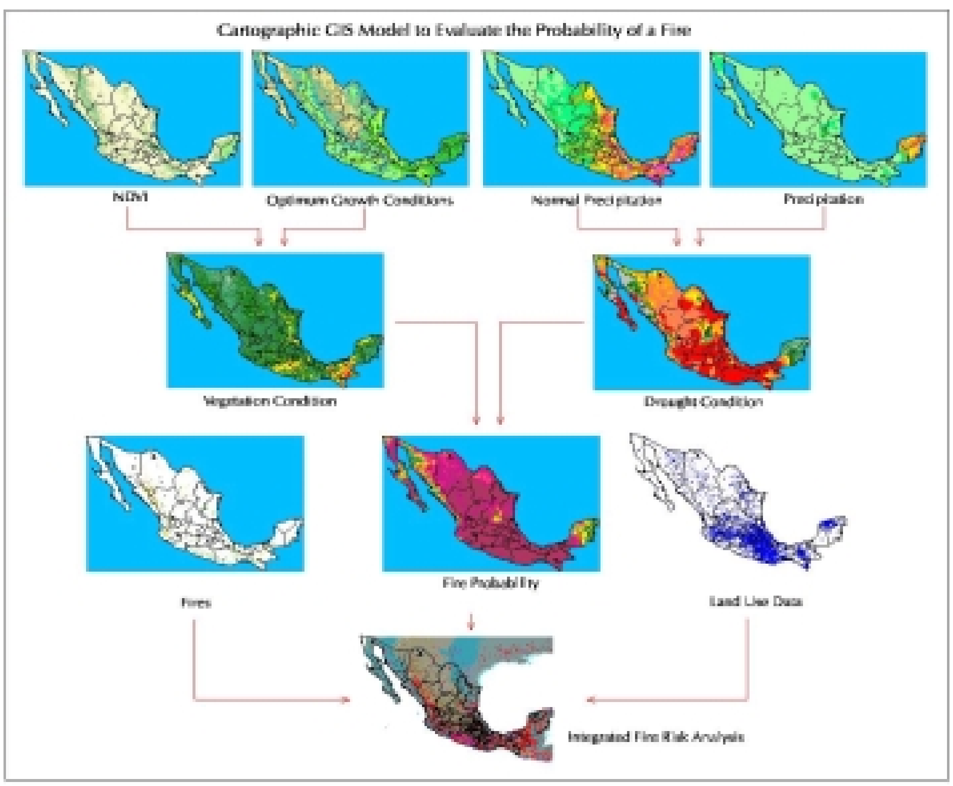

Figure 1. Cartographic GIS model to evaluate the “natural” probability of a fire in Mexico. The GIS model integrates multi-temporal satellite data to evaluate the vegetation condition, and drought information is derived from precipitation data.

ability of a fire requires then the use of monthly precipitation and "normal" precipitation data.

In model (1), fire probability is also directly associated with the "greenness", or conversely, with the "dryness" of the vegetation fuels. Fuel conditions are indirectly evaluated as a function of the vegetation condition, i.e., based on how dry or "green" the vegetation is under current conditions due to water stress.

The "greenness" condition is determined by analyzing the levels of photosynthetic activity that can be reached at a particular date. Then, the current vegetation condition is compared with historical levels of photosynthetic activity that can be reached under "optimal conditions" for vegetation growth (i.e., the maximum levels of photosynthetic activity observed during a period of observation for the healthiest, "greenest" vegetation). Both, the relative "greenness" and the "optimal conditions" can be only determined when several years of remotely sensed data are available. For that reason, patterns of "greenness" in the landscape can be determined only by multi-temporal satellite information.

Multi-temporal images from the Advanced Very High Resolution Radiometer (AVHRR) sensor, portraying the normalized difference vegetation index (NDVI), are frequently used to measure the vegetation condition over regional landscapes. The information derived from NDVI-AVHRR images has proven to be very useful for analyzing and characterizing vegetation patterns and land cover on a regional basis (Goward *et al.*, 1985, Justice *et al.*, 1985, Loveland *et al.*, 1991; Mora and Merchant 1996; Townshend *et al.*, 1985; Townshend *et al*., 1991) and particularly for Mexico (Mora and Iverson 1997).

Multi-temporal AVHRR-NDVI imagery can be used to evaluate the vegetation condition by calculating a measure of vegetation variability. Here, the *coefficient of greenness variation* (CGV) is a measure of the relative greenness vegetation condition (in percent) that is calculated when current NDVI values are compared with the historical NDVI levels for data that represent a determined period of observation.

$$CGV = NDVI_{std} / NDVI_{mean} \qquad (3)$$

Where:

$NDVI_{std}$ = the standard deviation of the photosynthetic level for a particular date ($NDVI_t$) and the "optimum growth" conditions ($NDVI_{op}$).

$NDVI_{mean}$ = the mean between the $NDVI_t$ and the $NDVI_{op}$

$NDVI_{op}$ is calculated as the maximum value for a long period of observation (e.g., 10 or more years).

Since CGV in (3) is compared with a historical NDVI maximum, high CGV values represent areas with vegetation stress, and low CGV values represent near-optimal vegetation growing conditions. For ENSO years in Mexico, higher deviations are expected to occur from optimal growth conditions because ENSO effects are primarily observed as droughts.

In addition, several sources of geographic data are integrated into the GIS fire potential model to calculate both sources of fire probability (i.e., vegetation and climate). A GIS layer representing different land cover categories is used to evaluate temporal and spatial patterns of fire potential for different ecological regions. Once fire probability is calculated for different regions, the fire potential is then compared with the incidence of actual fires.

Fire incidence can be obtained by different sources of satellite information such as thermal-infrared information from the AVHRR-NOAA satellites (Setzer and Malingreau 1996). The U.S. Air Force Defense Meteorological Satellite Program (DMSP) data also provides a reliable, independent source of information for fire potential validation (Eldvidge et al. 1996).

Sources of Data

At present, there are several sources of remotely sensed information that can be used for the analysis of fire potential at regional scales. Multi-temporal AVHRR-NDVI imagery can be used to evaluate vegetation fuels at different temporal scales (Burgan *et al.*, 1996; Burgan *et al* 1998), which when combined with climate data, offers the possibility to evaluate with GIS methods the "natural" probability of fire.

The imagery developed for the AVHRR-NDVI NOAA/NASA Pathfinder data (Belward *et al*., 1995; Smith *et al*., 1997) and the AVHRR-1km Global Land Dataset (Eidenshink 1990; Eidenshink and Faundeen 1994; Loveland *et al.*, 1991) were used as the primary sources of historical vegetation activity information. The AVHRR-NDVI Pathfinder data used here was produced from atmospheric corrected and calibrated daily AVHRR data from the operational meteorological satellites (NOAA-7, -9, -11) covering the period from 1982-1992. Multi-temporal NDVI imagery was available as 10-day composites, at 8-km resolution. The 1-

km Global AVHRR-NDVI data were derived from AVHRR-LAC daily data, and were available in 14-day composited images for the period 1992-1993 and 1995-1996. Data for 1998 were obtained from daily AVHRR-HRPT and AVHRR-LAC level-1b archived data (Satellite Active Archive, SSA-NOAA).

Precipitation data was obtained from weather observations gathered in ground stations in Mexico. Monthly mean precipitation data for the years 1982-1998, and long-term average (normal) precipitation data were integrated into a GIS by creating interpolated surfaces in mm per month with kriging methods.

Pre-processing 1998 AVHRR data

Daily NOAA-14 level-1b HRPT and LAC data for May of 1998 was obtained from the NOAA AVHRR Satellite Active Archive (SAA-NOAA). Daily, non-calibrated, unregistered AVHRR data was calibrated using the methodology proposed by Rao (1993a; 1993b) with a new set of calibration coefficients (Rao 1998).

The Normalized Difference Vegetation Index (NDVI) was calculated from calibrated, unregistered, and unrectified AVHRR data. The NDVI is related to the proportion of photosynthetically absorbed radiation by looking at the difference between the red and near-infrared channels of the AVHRR sensor. The NDVI is calculated from atmospherically corrected reflectance as:

$$NDVI = (NIR - RED) / (NIR + RED) \qquad (4)$$

Where RED is the reflectance in the visible wavelengths (0.58-0.68 μm) and NIR is the reflectance in the reflective infrared wavelengths (0.725-1.1 μm). The principle behind this band transformation is that RED reflectances are monitored in a part of the spectrum where chlorophyll causes considerable absorption of incoming radiation, and the NIR band is monitored in a spectral region where spongy mesophyll leaf structure leads to considerable reflectance (Tucker 1979; Tucker and Sellers 1988).

Atmospherically corrected and calibrated NDVI daily imagery were geo-corrected and geo-registered to a Lambert-Azimuthal Equal Area Projection. From calibrated, geo-corrected and geo-registered AVHRR-NDVI data, images for the maximum monthly value composites were obtained using ARC/INFO GRID software.

The Coefficient of Greenness Variation

Measures of vegetation activity were derived from multi-temporal observations of AVHRR-NDVI to provide an indication of the quantity of live vegetation. Imagery portraying the NDVI at a particular date, and was used to calculate the proportion of live fuel load (Burgan *et al.*, 1996, Burgan *et al.*, 1998).

The relative fuel conditions were determined here by comparing the current photosynthetic levels with the "optimal" growth conditions. The NDVI "optimum" vegetation condition was determined by calculating the maximum NDVI value for each month during a considerable long period (e.g., more than 10 years). In this case the "optimal growth conditions" represent maximum values calculated from a period comprising 1982 to 1998.

The relative greenness condition was then calculated using the coefficient of greenness variation (CGV), which is the coefficient of variation between the optimum and current NDVI monthly data for each year. The CGV is a measure of greenness variation similar to other relative greenness measures, where the CGV gives an indication of how green the vegetation is compared to how green it has been historically (Burgan and Hartford 1993).

Fire Mapping

Fire occurrence data were obtained from the U. S. Air Force Defense Meteorological Satellite Program (DMSP). The DMSP Operational Linescan System (OLS) has the capability to detect fires at night in a light intensified visible channel. DMSP currently operates OLS instruments aboard two satellites in day-night orbits (Satellites F12 and F14). Mexican fires were obtained from daily OLS-F14 images from May 23 to May 31, 1998 (Eldvidge *et al*. 1996).

Daily fire occurrences were summarized as a monthly composited image of fires by using ARC/INFO GRID software. Fire occurrences (pixel-fires) were converted to "fire patches" by connecting all fire-pixels that share a common border in an 8 by 8 window (eight nearest neighbors) using the REGIONGROUP command in arc/info GRID.

Ancillary Information

Population and socioeconomic data was implemented into a GIS as point coverage containing the location of all population centers in Mexico (CIESIN, 1999). The most recent land cover map available for the country (INEGI 1999) was used as a way to stratify the analysis. Thirty eight Land cover and vegetation classes were merged into a new classification containing 15 new generalized classes (agriculture, desert shrubland, grasslands, coniferous forest, deciduous forest, mixed forest, tropical rainforest or selvas, and different mosaics of the previous classes and secondary vegetation). All layers were converted into a raster format at 1 km spatial resolution.

Statistical Analysis for Model Validation

The number of fire (patch) occurrences (NF), the fire patch size (FPS), and the proportion of area affected with fires (PAF) within every land cover patch, were calculated with GIS functions by overlaying land cover map. Similarly the vegetation condition (VC), fire probability (FP), the size of every land cover patch (LCPS), and number of population centers (NPC) within every land cover patch were calculated with GIS zonal functions.

Multiple regression analysis was used to test the significance of the relationship between all fire variables (NF, FPS, PAF) and independent geographic variables (VC, FP, LCPS, NPC). Regression models were tested at statistical significance levels ($\alpha < 0.001$).

RESULTS & DISCUSSION

Fire Mapping

The dynamics of fire occurrences in Mexico is a response of different factors. Most of the wildfires are human induced and associated with land use practices. Fire occurrences cannot be considered just the result of natural causes. The geographic distribution of fires in Mexico mapped with OLS-F14 during the period of May 23 to May 31 is presented in Figure 2. The locations identified with OLS imagery represent fires that were observed with night-time imagery, so fires from agricultural burns (that usually occur during the day) were mostly excluded. Locations of contiguous fire pixels were used to define several “fire patches”, and their dynamic was monitored on daily basis. All fire patches observed daily were then merged into a monthly fire GIS coverage. A total number of 2052 fire patches distributed in Mexico were identified.

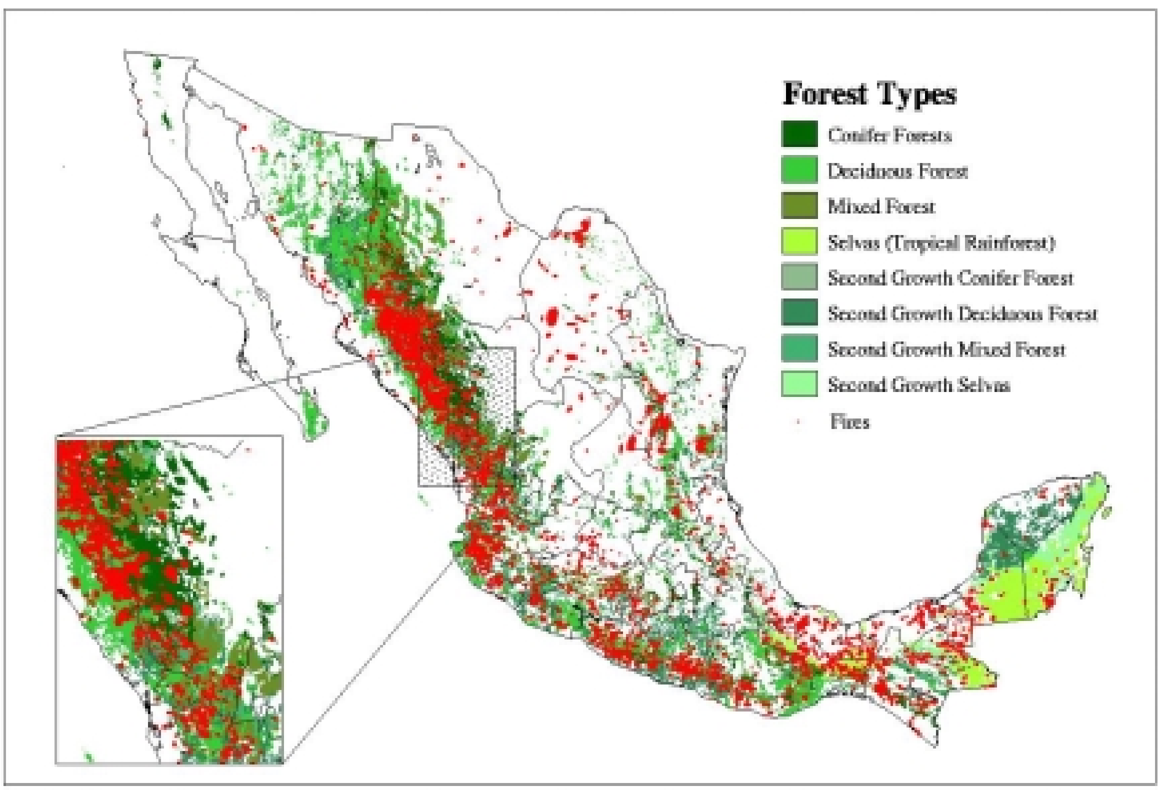

Figure 2. Fire occurrences observed with DMSP operational Linescan system OLS-F14 within each forest types in Mexico during May 23-31, 1998.

Most of the fire activity was concentrated along the Sierras (*Madre Oriental*, *Madre Occidental* and *Madre del Sur*) and tropical areas in Oaxaca and Chiapas. Fire patches were identified in the Mexican landscape varying from 1 to 5960 km^2. The average fire patch size was 44.33 km^2. The daily behavior of new appearing fires contiguous to previous pixel fires also indicated fire growth.

Characteristics of Mexican Fires

An overlay GIS analysis with ancillary land-cover data served to identify what vegetation types were most affected by these fires. The greatest fire activity was observed for areas with natural vegetation, mainly mixed forest (pine-oak forest) and deciduous forest (oaks). Fires in agricultural areas had an important proportion of fires observed with OLS imagery. Fire frequency in agricultural areas was similar to that observed for a mosaic of vegetation (deciduous tropical *matorrals* and *selvas*, mesophyllous forests, and agriculture) and shrublands, but was greater than the frequency observed for tropical forests (Figure 3).

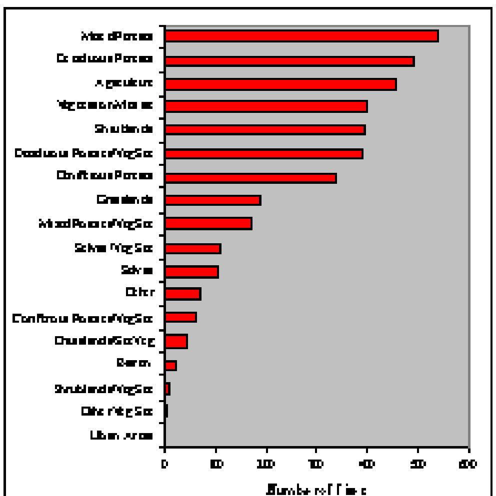

Figure 3. Incidence of fires observed with OLS-F14 imagery by land cover types in Mexico during May 23-31, 1998

The area affected by these fires varies also for each of the land cover types used for the analysis. Once again, Mixed forest (conifers-oaks), deciduous forest (including temperate deciduous and deciduous selvas) and coniferous forest (pines) were the most affected, as measured either by the total number or area burnt (Figure 4).

An analysis of average fire-patch size (Figure 5) indicated that fires have similar characteristics in areas with natural vegetation (e.g., grasslands, deciduous, mixed and coniferous forest). The average patch size in natural areas was ~30 km^2, while fire patches in agricultural and areas with secondary vegetation tended to be smaller (~15 km^2).

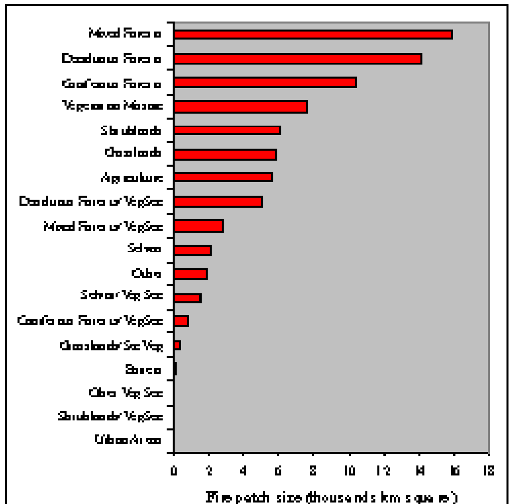

Figure 4. Area burned statistics for fires observed with OLS-F14 imagery by land cover type in Mexico during May 23-31, 1998

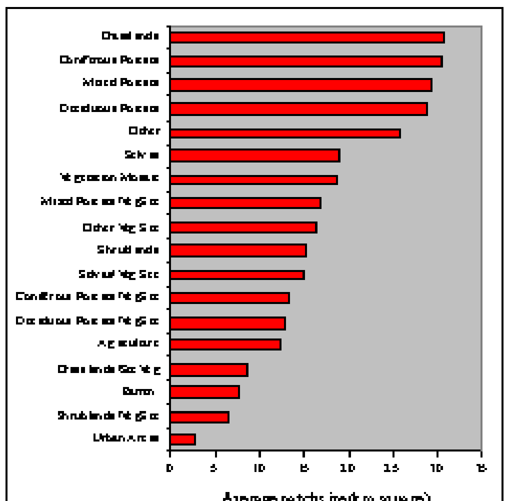

Figure 5. Fire patch characteristics observed with OLS-F14 imagery by land cover type in Mexico during May 23-31, 1998

Further GIS analysis of the spatial configuration of the location of fires, in relation with ancillary data (population centers and previous fires) revealed additional fire characteristics. Fires that occurred in natural areas were usually located near to human settlements. A great number of fires occurred especially in large forested patches and in areas not previously burned.

Vegetation Condition

The greenness vegetation condition during May of 1998 showed high levels of variation (expressed as percentage), as compared with the historical greenness values. High values of CGV indicated very dry conditions for most of the country, particularly in the savanna / grasslands of Chiapas and the Balsas region (southern Mexico). There was a good correspondence between fire locations and vegetation condition identified with AVHRR-NDVI imagery.

Several fires occurred in areas with greatest variation from the "optimal" growth conditions (i.e., greater dryness), indicating a strong correspondence between the vegetation condition and fire incidence (Figure 6). The analysis for the temporal variability of CGV indicated areas where vegetation condition was unusually dry (Figure 7).

The unusual dry vegetation conditions observed during 1998 were not totally unprecedented since similar dry conditions were observed for previous years (1982, 1983, 1987, 1988); with deviation values (CGV) greater than 50% for some areas. The levels and extent of the 1998 drought (measured as deviations from the historical greenness levels) is, however, only comparable to the conditions registered during 1982. During 1982 and 1998, drought conditions prevailed for most of the country, and were coincident with the occurrence of strong ENSO events. Conversely, the years in which levels of photosynthetic activity were similar to the "optimum" levels were 1984, 1992 and 1993.

A temporal analysis of the average vegetation condition also permitted to characterize the drought effects of ENSO for each land cover type. There is a differential response of vegetation to drought conditions (Figure 8). In general, shrubland and grassland vegetation types are more sensitive to variations in photosynthetic levels due to drought conditions (departure levels ~30% or greater) than temperate and tropical forests (20-30%), but all vegetation types responded similarly to the warm ENSO episodes, with significant high departures from the "optimal" greenness.

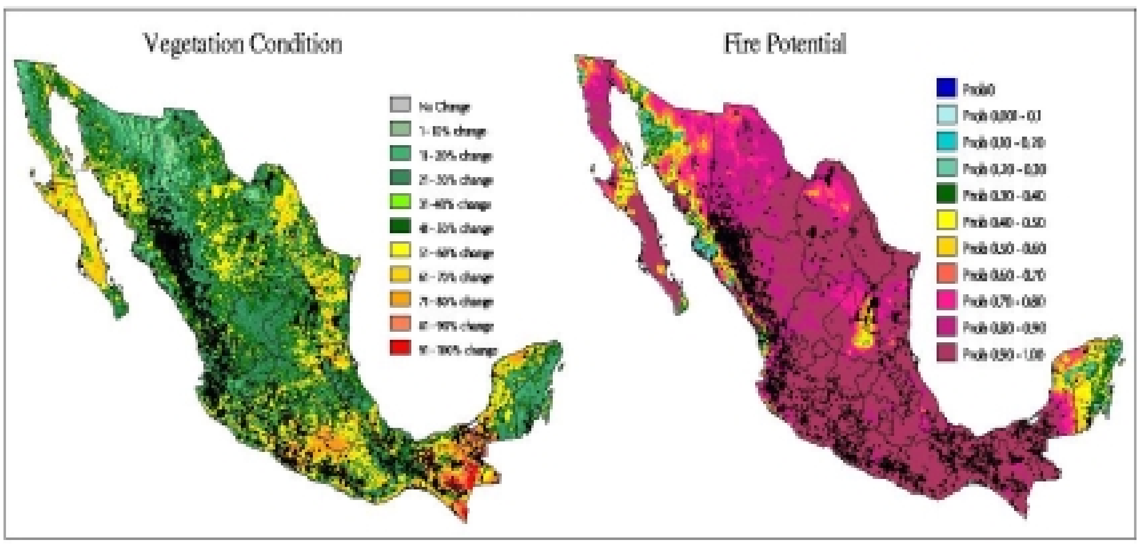

Figure 6. Vegetation condition estimated from multitemporal AVHRR-NDVI imagery, and fire potential estimated with a GIS model in relation with fire occurrences observed with OLS-F14 in Mexico during May 23-31, 1998.

Fire Potential

The maps resulting from the application of the probabilistic model for May, 1998 showed the areas with the apparent highest fire potential in the country (Figure 9). Similarly to what was observed for vegetation condition, there was also a good agreement between the location of DSMP-OLS fires and high fire probabilities. Most of the fires occurred in areas where the GIS model predicted high potential for fire development.

The effects that ENSO may have in modifying the natural probability of a fire were only identified when several years of data were compared. The analysis of the vegetation condition and the fire probabilities during the driest month of the year helped to elucidate "El Niño" effects. These effects are primarily regional,

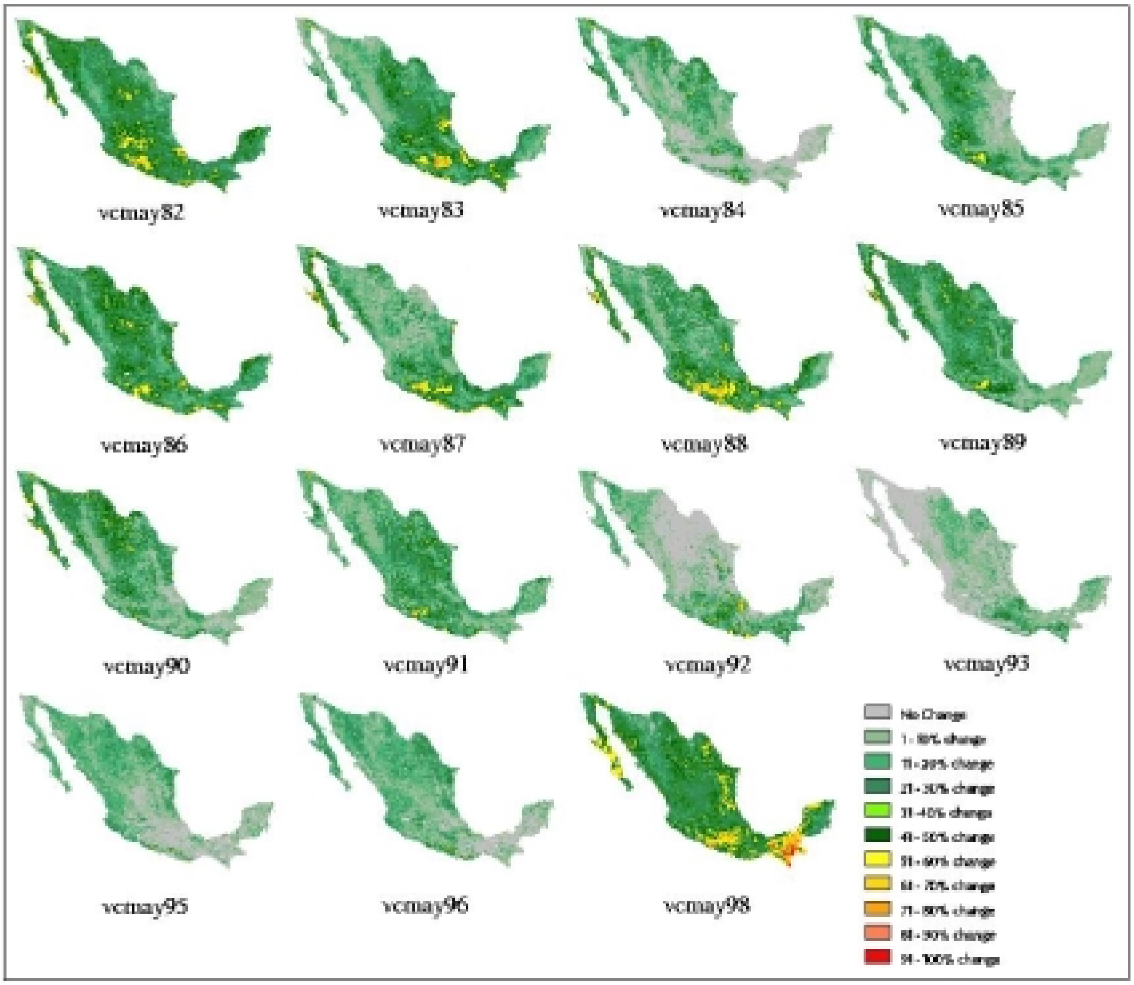

Figure 7. Vegetation condition, measured as the coefficient of greenness variation (CGV) estimated from multi-temporal AVHRR -NDVI imagery from 1982 to 1998.

affecting similarly all land cover types and can be monitored consistently with AVHRR imagery.

Fire severity occurring during May of 1998 had a strong relationship with the occurrence of warm phases of "El Niño". It is clear that ENSO activity can take the severity of fires to catastrophic levels, due to lack of precipitation and unusual dry vegetation conditions. The inter-annual pattern variation observed in fire potential also showed that the interaction between vegetation and drought conditions create different patterns of fire risk for the country, when the climatic conditions are considered in the model. Lack of precipitation can also play a big role in determining fire probability (as observed for the years 1986 and 1998).

Validation of the Fire Potential GIS Model

We tested the contribution of several factors in explaining fire severity during 1998, and we evaluated if fire damage could be directly associated with natural conditions as monitored with satellite images. We observed that fuels could rapidly build-up due to drought conditions favoring fire risk as calculated by the GIS model. We tested the relationship between vegetation conditions, the number of fires and fire damage (area burned).

There was a significant relationship between fire variables (e.g., NF, FPS, and PAF) and factors that promote forest fire occurrences. Various combinations of the independent variables accounted for ~50 to 95% of the variation in the fire variables.

The results of regression analysis showed that the number of population centers within forested areas (NPC); land cover patch size (LCPS) and vegetation condition (VC) explained more than 50% of the variance in the number of forest fires (NF) observed with satellite imagery ($R2 = 0.540$, $p < 0.001$). The model that

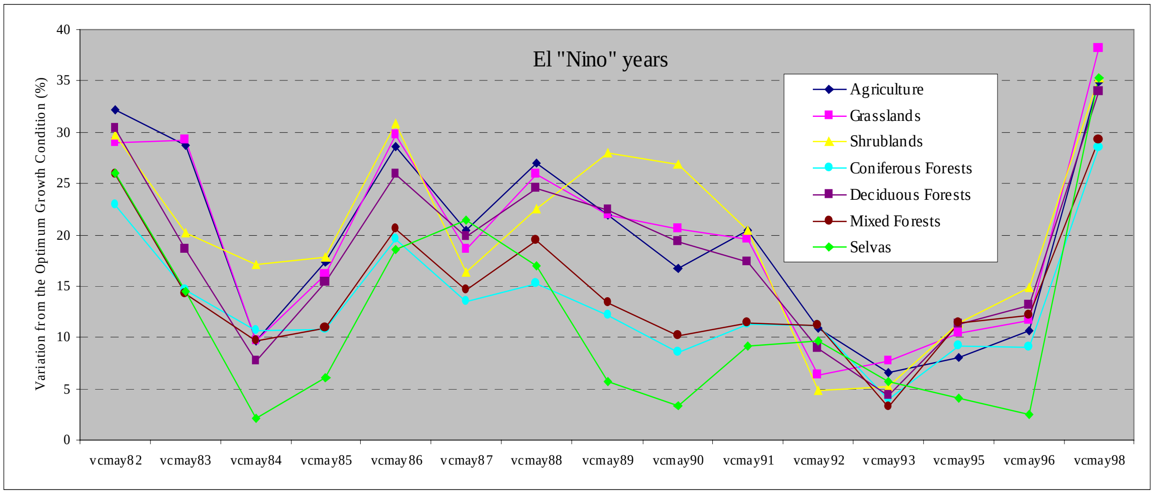

Figure 8. Temporal variation of the vegetation condition (GVC) for different land cover types in Mexico, derived from multi-temporal AVHRR/NDVI imagery.

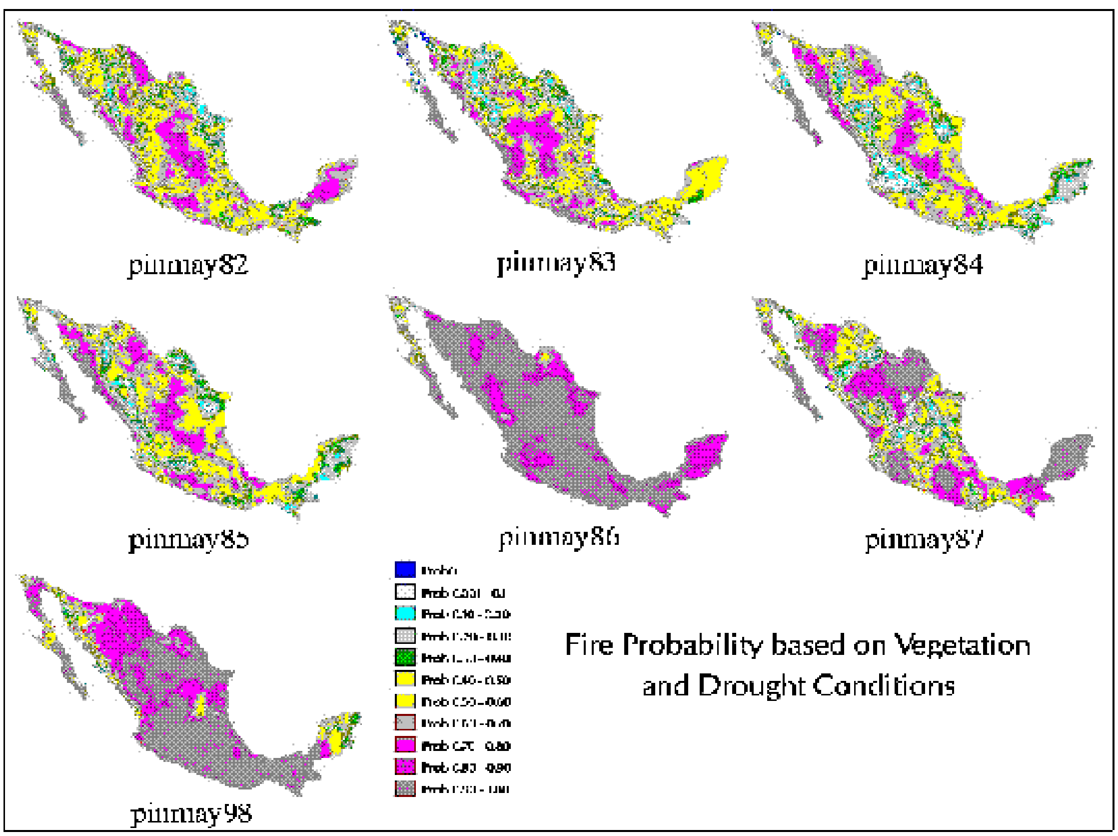

Figure 9. Inter-annual variations in fire potential from multi-temporal AVHRR-NDVI imagery and a GIS probabilistic model from 1982 to 1998.

describes the relationship is:

NF = 3.16 + 0.1690 (NPC) + 0.0009 (LCPS) - 0.035 (VC)

Where the number of forest fires increased as the values NPC and LCPS increase and slightly decreased with VC. In other words, the greater number of population centers within a forest patch, and the greater the forest patch area, the greater number of fires occurred within a forest patch (Figure 10).

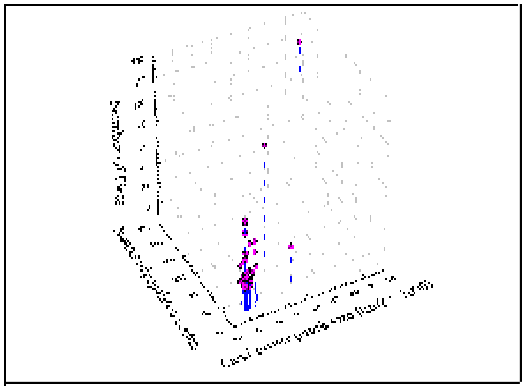

Figure 10. Relationship between number of fires (NF), number of population centers (NPC) and land cover patch size (LCPS) for forested areas in Mexico.

The area affected by fires within each forest patch (FPS) was also significantly correlated with the independent variables. More than 88% of the variation of the area affected by fires within forest patches was significantly explained ($R^2 = 0.886$, $p < 0.001$) by the variation of NPC, LCPS and VC. The parameters for the regression model are:

$$FPS = 17.67 + 13.13\,(NPC) + 0.036\,(LCPS) - 1.11\,(VC)$$

According with this model, the area affected by fires increases as the number of population centers and the land cover patch size increases (Figure 11).

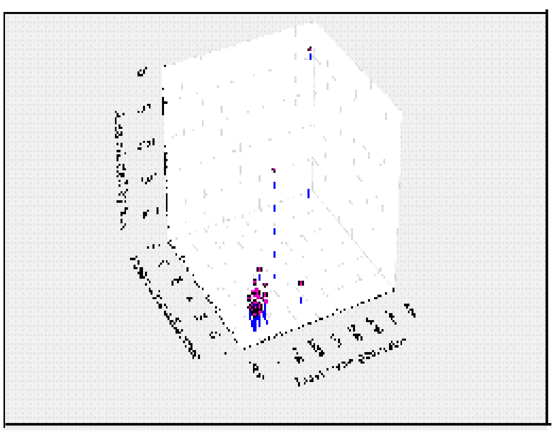

Figure 11. Relationship between area affected by fires (FPS), number of population centers (NPC) and land cover patch size (LCPS) for forested areas in Mexico.

The contribution of the vegetation condition (VC) was significant ($p < 0.001$) to explain the variation of NF and FPS in all models tested. Fire probability was not significant in any model. The lack of correlation between the number of forest fires and vegetation condition can be partially explained by fire control practices (most of the fires were actively suppressed during April and May).

CONCLUSIONS

We tested the hypothesis that the occurrence of the strongest "El Niño" Southern Oscillation (ENSO) event in the century was the major driving factor in determining fire severity during 1998. "El Niño" produced severe drought conditions for most of the country since the summer season of 1997, and the worst effects were produced during May 1998. During June to September 1997, ENSO activity resulted in a strong suppression of the tropical storm activity in the Gulf of Mexico. Lack of rain, and unfavorable meteorological conditions, created an unusual drought that affected most of the country, with water deficits reaching more than 500 mm on some areas of Mexico (NOAA 1998).

"El Niño" reached its peak at the beginning of the 1998 spring season, causing the most severe, ever-recorded drought for the country in the last 50 years. Drought conditions favored an unusual build-up of natural fuels, increasing dramatically the potential for fire development. Since February 1998, between 50-60 fires were reported each day. During May, more than 500 fire-patches were observed with satellite OLS imagery on daily basis, most of them burning out of control. The location of those fires corresponded well with the predictions of our fire model. We conclude that this model can be used to identify areas with greater risk.

Fire severity was evaluated by using both the number of fires and the area affected by fires, and correlated with natural conditions. However human activity is significantly related with both, the number of fires and area burned. The areas most affected by fires were natural areas, primarily forests. Wildfires occurring in the Mexican landscape seemed mainly associated with deforestation practices. There is a general tendency to believe that most fires occur as a result of agricultural practices (i.e., agricultural burns) and are not intended to promote land use changes. However, most of the fires detected with DMSP-OLS imagery occurred predominantly in forested areas. Coniferous and mixed forests were the most affected types.

Fire frequency in forested areas reinforces the idea that the use of fire is a main tool for deforestation, especially in large forest patches. The greater the forest-patch area, the greater the probability that a fire can be initiated. The greater the CVG the greater the area affected by fires.

Satellite imagery was also proven very useful to identify trends in vegetation condition and ENSO activity. The vegetation condition was always unusually dry for years with warm ENSO phases for all the land cover types considered in this analysis. During “mild” ENSO events, high potential for the development of fires is spatially heterogeneous, with the highest risks located in several (and extensive) areas throughout the country, depending upon the interaction of vegetation condition and lack of precipitation. Conversely, for “strong” ENSO events, the probability of fires expands dramatically for almost the totality of the territory having as a result a catastrophic occurrence of fires, in both number and area affected.

Fire severity, however, is a direct result of human practices and population size. An extensive analysis of fire activity that integrates the use of socio-economic data seems necessary.

ACKNOWLEDGEMENTS

This research was conducted while the second author was supported as a visitor scientist for the Center for Advanced Land Management Information Technologies (CALMIT) University of Nebraska - Lincoln.

REFERENCES

Andreae, M. O. 1991. Biomass burning: Its history, use and distribution and its impacts on environmental quality and global climate. In J.S. Levine (ed.) *Global biomass burning: Atmospheric, climatic, and biospheric implications*. The MIT Press, Cambridge, Massachusetts, 3-21.

Barbosa, P. M., J. Gregoire, and J. M. C. Pereira. 1999. An algorithm for extracting burned areas from time series of AVHRR GAC data applied at a continental scale. Remote Sensing of the Environment 69: 253-

Belward, A., A. Hoolyfield, and M. James. 1995. The potential of the NASA GAC pathfinder product for the creation of global thematic data sets: the case of biomass burning patterns. *International Journal of Remote Sensing* **16**: 2089-2097.

Burgan R. E., R. A. Hartford, and J. C. Eidenshink. 1996. Using NDVI to assess departure from average greenness and its relation to fire business. USDA Forest Service, Intermountain Research Station. *Gen. Tech. Report* INT-GTR-333.

Burgan, R. E.; R. W. Klaver, and J. M. Klaver. 1998. Fuel models and fire potential from satellite and surface observations. *International Journal of Wildland Fire* **8** (3): 159-170.

Burgan, R. E., and R. A. Hartford. 1993. Monitoring vegetation greenness with satellite data. USDA Forest Service, Ogden UT. *Gen. Tech. Rep*. INT-297.

Chuvieco E. and R. G. Congalton. 1989. Application of remote sensing and geographic information systems to forest fire hazard mapping. *Remote Sensing of Environment* **29**: 147-159.

Chuvieco E. and P. Martin. 1994. Global fire mapping and fire danger estimation using AVHRR images. *Photogrammetric Engineering & Remote Sensing* **60**: 563-570.

Chuvieco E. and J. Salas. 1996. Mapping the spatial distribution of frorest fire danger using GIS. *International Journal of Geographical Information Systems* **10**: 333-345.

CIESIN, 1999. Georeferenced Population Database for Mexico, prepared by CIESIN, Center for International Earth Science Information Network, Columbia University, New York.

Ehrlich, D. E. F. Lambin, and J. Malingreau. 1997. Biomass burning and broad-scale land cover changes in western Africa. *Remote Sensing of Environment* **61**: 201-209.

Eidenshink. 1990. The 1990 conterminous U. S. AVHRR data set. *Photogrammetric Engineering &Remote Sensing* **58**: 809-813.

Eidenshink, J. C. and J. L. Faundeen. 1994. The 1 km AVHRR global land data set: first stages in implementation. *International Journal of Remote Sensing*. **15**: 3443

Eldvige, C. D. H. W. Kroehl, E. A. Kihn, K. E. Baugh, E. R. Davis and W. M. Hao. 1996. Algorithm for the retrieval of fire pixels from DMSP operational linescan system data. In, Levine J. S. (ed.) *Biomass burning and global change*. The MIT Press, Cambridge Massachussets. Pages 73-85.

Goward, S. N., C. J. Tucker, and D. Dye. 1985. North American vegetation patterns observed with NOAA-7 advanced very high resolution radiometer. *Vegetatio* **64**: 3-14.

Hao, W. M. and M. H. Liu. 1994. Spatial and temporal distribution of tropical biomass burning. *Global Biochem. Cycles* **8**: 495-503.

Hugh, E. and E. F. Lambin. 1998. Remote sensing of biomass burning in tropical regions: sampling issues and multi-sensor approach. *Remote Sensing of Environment* **64**: 292-315.

INEGI, 1999. Land Use and Vegetation Map Serial 1 (Carta de uso de suelo y vegetación, Serie 1), escala 1: 1 000 000. Instituto Nacional de Geografía Estadística e Informática. Mexico.

James, M. E. and S. N. V. Kalluri. 1994. The Pathfinder AVHRR land data set: An improved coarse resolution data set for terrestrial monitoring. *International Journal of Remote Sensing*. 5: 3347.

Justice, C. O., J. R. G. Townshend, B. N. Holben, and C. J. Tucker. 1985. Analysis of the phenology of global vegetation using meteorological satellite data. *International Journal of Remote Sensing*, **6**:1271-1318.

Levine, J. S., T. Bobbe, N. Ray, R. G. Witt, and A. Singh. 1999. Wildland fires and the environment: A global synthesis. Environment information and assessment technical report 1. UNEP / DEIA & EW / TR.99-1.

Loveland, T. R., J. W. Merchant, D. O. Ohlen, and J. F. Brown. 1991. Development of a land-cover characteristics database for the conterminous U. S. *Photogrammetric Engineering & Remote Sensing* **57**: 1453-1463.

Mora, F., and J. W. Merchant. 1996. Exploring the inter-annual variation of vegetation activity using multi-temporal AVHRR/NDVI Images. Pages in the 1996 *International Geoscience and Remote Sensing Symposium: Remote sensing for a sustainable future*. May 27-31 Lincoln, Nebraska, USA.

Mora, F. and L. R. Iverson. 1997. Dynamic stratification of the landscape of Mexico: analysis of vegetation patterns observed with multi-temporal remotely sensed images. *Geocarto International* **12**: 73-88.

NOAA 1997. Climate conditions associated with El Niño: impacts and outlook. Special climate summary 97/3. November 1997. Climate Prediction Center, NOAA.

Rao, C. R. N. 1993a. Nonlinearity corrections for the thermal infrared channels of the Advanced Very High Resolution Radiometer: assessment and recommendations. NOAA Technical Report NESDIS-69. NOAA/ NESDIS. Washington, DC.

Rao, C. R. N. 1993b. Degradation of the visible and near-infrared channels of the Advanced Very High Resolution Radiometer on the NOAA-9 spacecraft: assessment and recommendations for corrections. NOAA Technical Report NESDIS- 70. NOAA/ NESDIS. Washington, DC.

Reed, B. C. 1993. Using remote sensing and Geographic Information Systems for analyzing. landscape/ drought interaction. *International Journal of Remote Sensing* 14: 3489.

Setzer, A. W. and J. P. Malingreau. 1996. AVHRR monitoring of vegetation fires in the tropics: Toward the development of a global product. In, Levine J. S. (ed.) *Biomass Burning and Global Change*. The MIT Press, Cambridge Massachussets. Pages 3-39.

SEMARNAP, Secretaria de Manejo de Recursos Naturales y Pesca. 1998. Acciones contra incendios forestales de 1998. CONAF (WWW document).

Smith, P. M., S. N. V. Kalluri, R. DeFries. 1997. The NOAA/NASA Pathfinder AVHRR 8-Km Land Data Set. *Photogrammetric Engineering & Remote Sensing* 63: 12.

Tucker, C. J. 1979. Red and photographic infrared linear combinations for monitoring vegetation. *Remote Sensing of Environment*, **8**:127-150.

Tucker, C. J. and P. J. Sellers. 1988. Satellite remote sensing of primary production. *International Journal of Remote Sensing* **7**: 1395-1416.

Townshend, J. R. G., C. Justice, W. Lei, C. Gurney, and J. McManus. 1991. Global land classificaction by remote sensing: Present capabilities and future possibilities. *Remote Sensing of Environment* **35**: 243-255.

Townshend, J. R. G., T. E. Goff, and C. Tucker. 1985. Multi-temporal dimensionality of images of normalized difference vegetation index at continental scales. *IEEE Transactions on Geoscience and Remote Sensing* **GE-23**: 888-895.